Supplementary: An Adaptable Dead Fuel Moisture Model for Various Fuel Types and Temporal Scales Tailored for Wildfire Danger Assessment

Nicolò Perello[a,b,*], Andrea Trucchia[b], Mirko D'Andrea[b], Silvia degli Esposti[b], Paolo Fiorucci[b], Andrea Gollini[c], Dario Negro[c]

[a] *Department of Informatics, Bioengineering, Robotics and Systems Engineering, University of Genoa, Via All'Opera Pia, 13, Genova, 16145, Italy*
[b] *CIMA Research Foundation, Via A. Magliotto, 2, Savona, 17100, Italy*
[c] *Dipartimento della Protezione Civile, Presidenza del Consiglio dei Ministri, via Vitorchiano 2, Roma, 00189, Italy*

1. Different Formulations of the Response Time

Different formulations for the response time has been tested, by selecting the one that performed better in the validation dataset of the no-rain samplings. Let recall that the response time K_i is defined as dependent of weather conditions i.e., temperature T $[°C]$, wind speed W $[m/s]$ and relative humidity H $[\%]$, by modifying the fuel-specific *standard response time* K_0:

$$K_i(T, W, H) = K_0 G_i(T, W, H) \qquad i = d,\, w \tag{1}$$

where $i = d$ stands for *drying* and $i = w$ stands for *wetting* processes. In fact, the response time depends on the process in which is considered, defined according to the initial condition with respect to the Equilibrium Moisture Content (EMC) - see the paper for more details. The standard response time

*corresponding author
Email addresses: nicolo.perello@edu.unige.it (Nicolò Perello), andrea.trucchia@cimafoundation.org (Andrea Trucchia), mirko.dandrea@cimafoundation.org (Mirko D'Andrea), silvia.degliesposti@cimafoundation.org (Silvia degli Esposti), paolo.fiorucci@cimafoundation.org (Paolo Fiorucci), Andrea.Gollini@protezionecivile.it (Andrea Gollini), Dario.Negro@protezionecivile.it (Dario Negro)

refers to standard weather conditions as defined by Nelson (2000) which are: $T_{st} = 27°C$, $W_{st} = 0\,m/s$, $H_{st} = 20\%$. To let the response time be equal to K_0 in case of standard weather conditions, the *dry/wet factor*:

$$G_i(T, W, H) = D_i g_i(T, W, H) \tag{2}$$

which accounts for weather contribution, is normalized to 1 in the standard weather conditions by D_i, so that

$$K_i(T_{st}, W_{st}, H_{st}) = K_0$$

Three different formulations of $g_i(T, W, H)$ have been tested during the calibration process, with different dependence on weather variables:

- F.1: same formulation for both drying and wetting processes, with inversely proportional dependence on wind and temperature:

$$g_i(T, W) = \frac{1}{1 + b_{1,i} T^{c_{1,i}} + b_{2,i} W^{c_{2,i}}} \qquad i = d,\ w \tag{3}$$

  Wind and temperature dependencies follow the Fine Fuel Moisture Code (FFMC) of the Fire Weather Index (FWI), while for the sake of simplicity no dependence on relative humidity has been considered;

- F.2: same formulation of F.1 for the drying process has been adopted, while the dependencies from the weather variables have been inverted in the wetting process:

$$g_d = \frac{1}{1 + b_{1,d} T^{c_{1,d}} + b_{2,d} W^{c_{2,d}}} \qquad g_w = (1 + b_{1,w} T^{c_{1,w}} + b_{2,w} W^{c_{2,w}}) \tag{4}$$

  In this case, temperature and wind favor the drying process and so reducing the response time in drying process (Pausas and Keeley, 2021), while it is increased during the wetting phase as the absorption process is contrasted;

- F.3: it is a modification of F.2 integrating the relative humidity H. In this formulation, H favors the wetting process and reduces the time of absorption, while it increases the drying time:

$$g_d = \frac{1 + b_{3,d} H^{c_{3,d}}}{1 + b_{1,d} T^{c_{1,d}} + b_{2,d} W^{c_{2,d}}} \qquad g_w = \frac{1 + b_{1,w} T^{c_{1,w}} + b_{2,w} W^{c_{2,w}}}{1 + b_{3,w} H^{c_{3,w}}} \tag{5}$$

Table 1: The table reports the Sum of Squared Residuals (SSR) values for the three different formulations proposed for the no-rain phase, tested on the no-rain validation dataset.

	$\phi = 0.2$	$\phi = 0.5$	$\phi = 0.8$
F.1	127992.9	125791.2	124219.5
F.2	52353.4	52214.3	54469.3
F.3	47307.5	47497.6	50275.3

The calibration process of the no-rain phase has been repeated for the three formulation, selecting the one that obtained the minimum objective function value in the no-rain validation dataset. As shown in Table 1, the formulation F.3 performed better - it was selected as final response time formulation of the DFMC model. The results are reported for the three values tested for the hyper-parameter *social learning probability* ϕ of the optimization algorithm MSL-PSO.

2. Further Analysis on the Calibration Datasets

In the following section, further statistical analysis of the calibration datasets is proposed. The fuel sticks information of the ISR dataset can be found in Table 2.

In Tables 3, 4 and 5 the mean, standard deviation, minimum and maximum values respectively for the rain, no-rain and mixed samplings of the ISR dataset are reported. The same analysis is proposed in Table 6 for the BC dataset. In Figures 1, 2 and 3 the month distribution of no-rain, rain and mixed samplings, respectively, are reported.

3. Results on No-rain and Rain samplings

In the following section, the results obtained on the no-rain and rain phases calibration processes are reported. In Figures 4 and 5 the comparison between observed and modeled fuel moisture values for the validation datasets of the no-rain and rain samplings are reported. In Table 7 the Goodness-of-Fit (GoF) measures obtained for the no-rain and rain samplings on validation datasets are reported. In particular, the GoF measures are computed for each time series samplings - the median, minimum and maximum values are reported in the Table. Also, in Figures 6 and 7 the GoF measures

Table 2: The table provides information on the five fuel sticks of the dataset from the Israel Meteorological Service (ISR dataset) and used for the model's calibration and validation. Specifically, it reports the location and altitude (Alt.) of each fuel stick, along with the time range of data, and the indices for completeness (Compl.) and continuity (Cont.) of the time series. The completeness index indicates the percentage of valid data available, while the continuity index reflects the presence of continuous intervals of valid data; both of the range in $[0, 1]$, where 1 refers to continuous and complete time series.

	Location	Lat.	Lon.	Alt.	Time range	Compl.	Cont.
ISR1	Afula Nir Haemeq	35.2769	32.596	60 m	2017/04/19 2021/06/01	0.81	0.99
ISR2	Gamla	35.7484	32.9056	405 m	2017/05/22 2021/07/21	0.80	0.99
ISR3	Nashon	34.9544	31.8308	180 m	2017/05/09 2021/07/21	0.85	0.99
ISR4	Zefat Har Knaan	35.507	32.98	936 m	2018/04/12 2021/07/21	0.68	0.99
ISR5	Zova	35.1203	31.7803	715 m	2017/04/04 2021/07/21	0.94	0.99

Table 3: Statistics on no-rain samplings from ISR dataset.

ISR dataset - No rain samplings				
	mean	**std**	**min**	**max**
Fuel moisture [%]	9.2	3.1	1.8	39.2
Relative humidity [%]	59.8	22.8	6.0	100.0
Temperature [$^{\circ}C$]	22.8	6.4	1.6	43.7
Wind speed [m/s]	2.9	1.8	0.0	14.0
Rain [mm]	0.0	0.0	0.0	0.0

are also reported through visual representation - each matrix corresponds to a different GoF measure, and each cell corresponds to a different time series samplings.

Table 4: Statistics on rain samplings from ISR dataset.

ISR dataset - Rain samplings				
	mean	**std**	**min**	**max**
Fuel moisture [%]	33.8	6.0	8.8	45.3
Relative humidity [%]	94.7	7.2	48.0	100.0
Temperature [$^{\circ}C$]	9.4	3.3	0.1	21.1
Wind speed [m/s]	4.8	3.3	0.5	19.9
Rain [mm]	2.0	2.4	0.1	22.2

Table 5: Statistics from mixed samplings from ISR dataset, divided between Summer and Winter clusters.

ISR dataset - Mixed samplings								
	Winter cluster				**Summer cluster**			
	mean	**std**	**min**	**max**	**mean**	**std**	**min**	**max**
Fuel moisture [%]	15.8	9.4	1.1	45.7	9.3	3.0	2.0	40.7
Relative humidity [%]	70.1	23.7	6.0	100.0	61.5	22.6	6.0	100.0
Temperature [$^{\circ}C$]	13.7	5.4	0.1	39.4	24.2	5.4	8.7	43.7
Wind speed [m/s]	3.34	2.4	0.0	20.2	2.8	1.7	0.0	16.5
Rain [mm]	0.1	0.8	0.0	20.2	0.0	0.1	0.0	10.6

Table 6: Statistics from the BC dataset.

BC dataset				
	mean	**std**	**min**	**max**
Fuel moisture [%]	13.5	6.9	4.8	37.7
Relative humidity [%]	63.1	24.9	10.5	99.7
Temperature [$^{\circ}C$]	14.1	7.6	-5.3	35.7
Wind speed [m/s]	0.6	0.3	0.3	2.0
Rain [mm]	0.0	0.3	0.0	6.8

4. Time Series Examples

In the following section, some examples of fuel moisture time series modeled and observed are reported, from the mixed sampling dataset. In par-

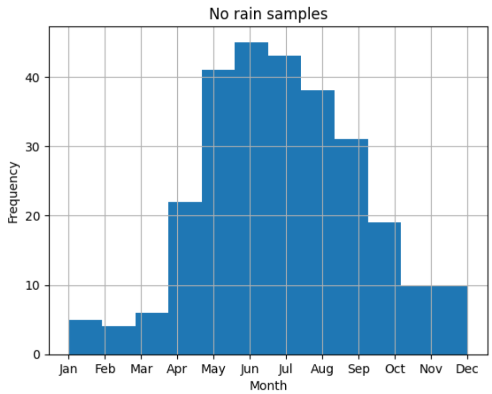

Figure 1: Month distribution of no rain samplings.

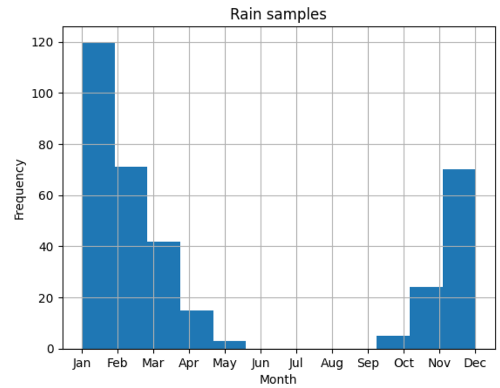

Figure 2: Month distribution of rain samplings.

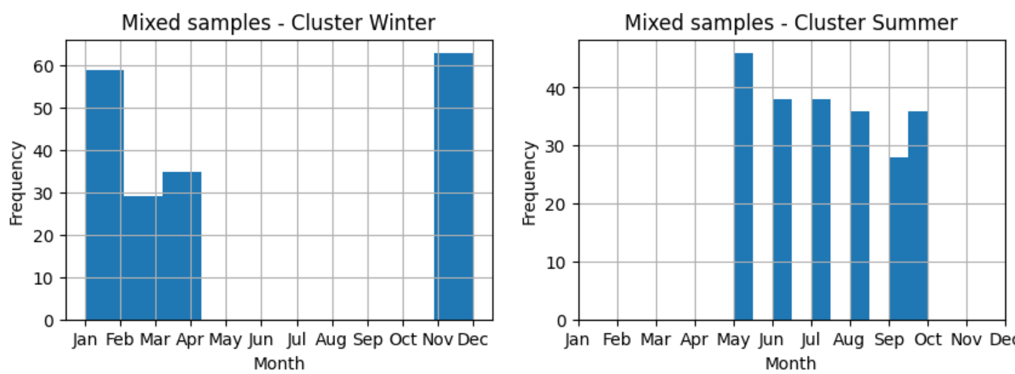

Figure 3: Month distribution of mixed samplings, divided in the two Winter and Summer clusters.

ticular, the best and worst simulated time series in terms of Mean Absolute Error (MAE) are reported for the Summer cluster (respectively Figures 8 and 9) and Winter cluster (respectively Figures 10 and 11).

References

Nelson, J., 2000. Prediction of diurnal change in 10-h fuel stick moisture content. Canadian Journal of Forest Research 30, 1071–1087. doi:10.1139/cjfr-30-7-1071.

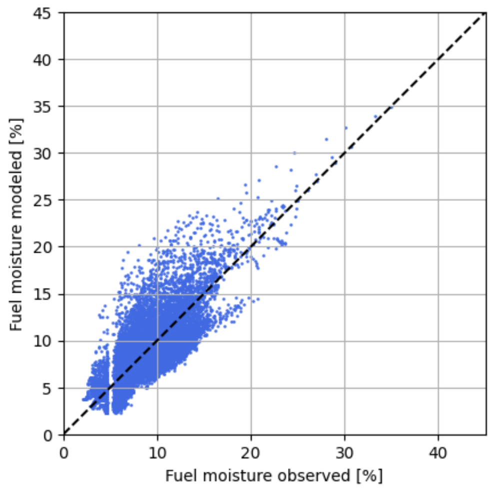

Figure 4: Comparison between observed and modeled fuel moisture values for the no-rain samplings.

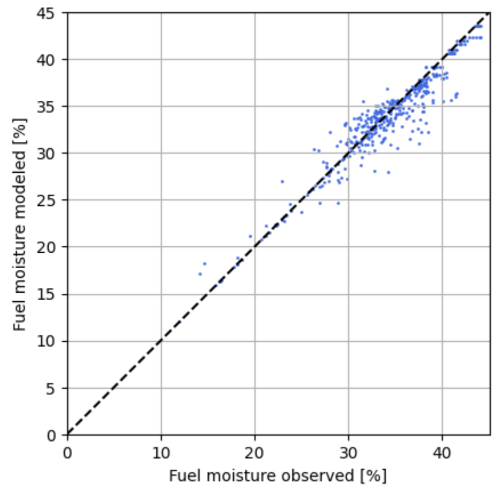

Figure 5: Comparison between observed and modeled fuel moisture values for the rain samplings.

Table 7: Goodness-of-Fit measures values for the no-rain and rain samplings from the ISR dataset.

ISR dataset (median-min-max)		
	No-rain	**Rain**
MAE [%]	1.48	0.86
	0.43	0.18
	5.0	4.28
BIAS [%]	-0.2	-0.3
	-3.17	-4.28
	5.05	3.22
RMSE [%]	1.78	1.06
	0.53	0.23
	5.9	4.69
NNSE *[adim]*	0.51	0.57
	0.07	0.16
	0.86	0.99

Pausas, J.G., Keeley, J.E., 2021. Wildfires and global change. Frontiers in

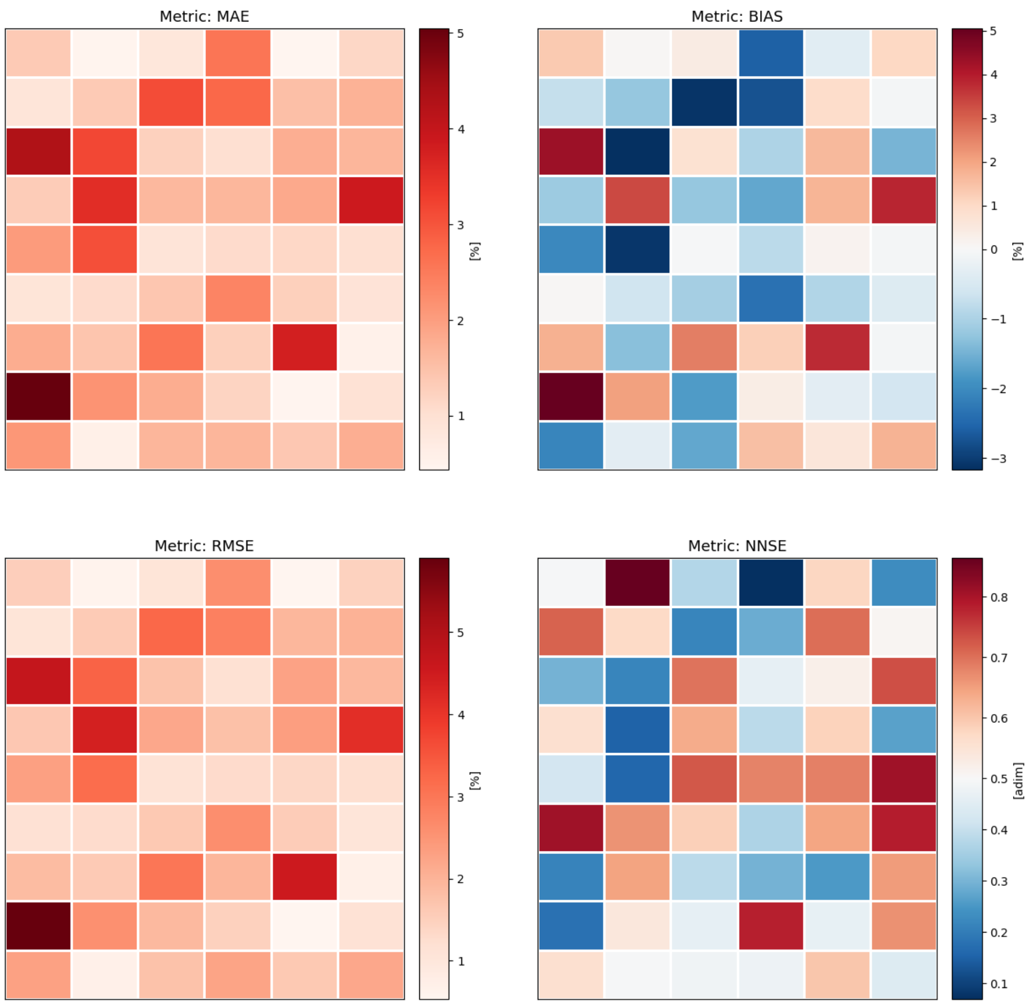

Figure 6: The matrices of the Goodness-of-Fit measures (MAE, Bias, RMSE, NNSE) obtained for the no-rain sampled time series. Specifically, each cell in each matrix corresponds to a different time series.

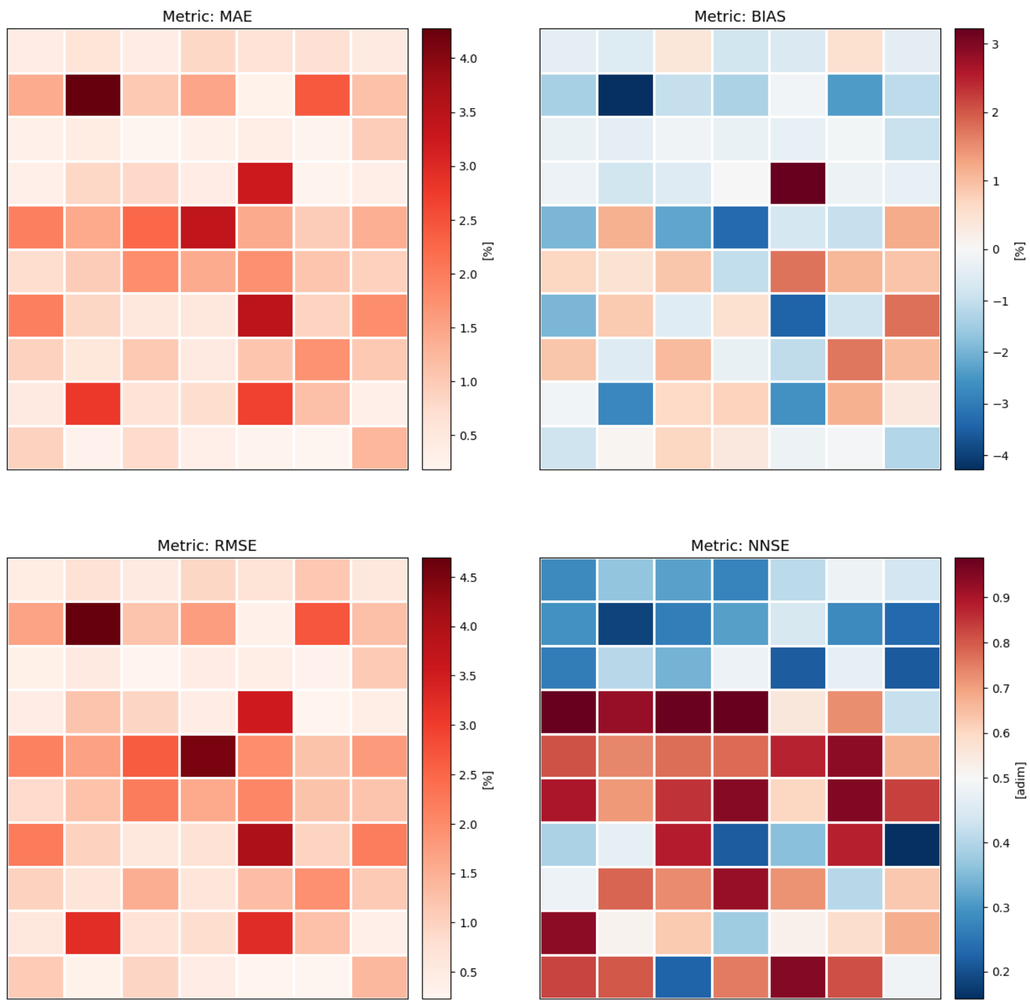

Figure 7: The matrices of the Goodness-of-Fit measures (MAE, Bias, RMSE, NNSE) obtained for the rain sampled time series. Specifically, each cell in each matrix corresponds to a different time series.

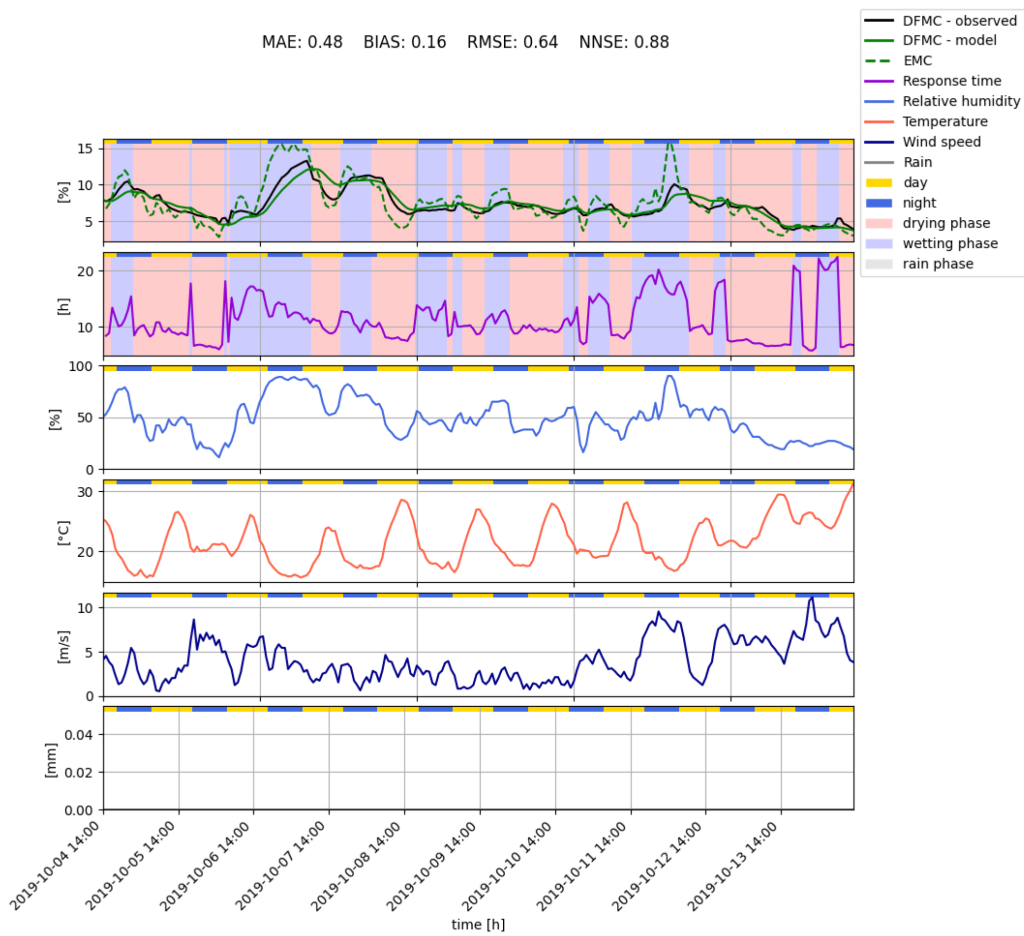

Figure 8: Mixed samplings, Summer Cluster - best time series in terms of Mean Absolute Error (MAE). The other Goodness-of-Fit measures (bias, Root Mean Square Error and Normalized Nash-Sutcliffe) are also reported.

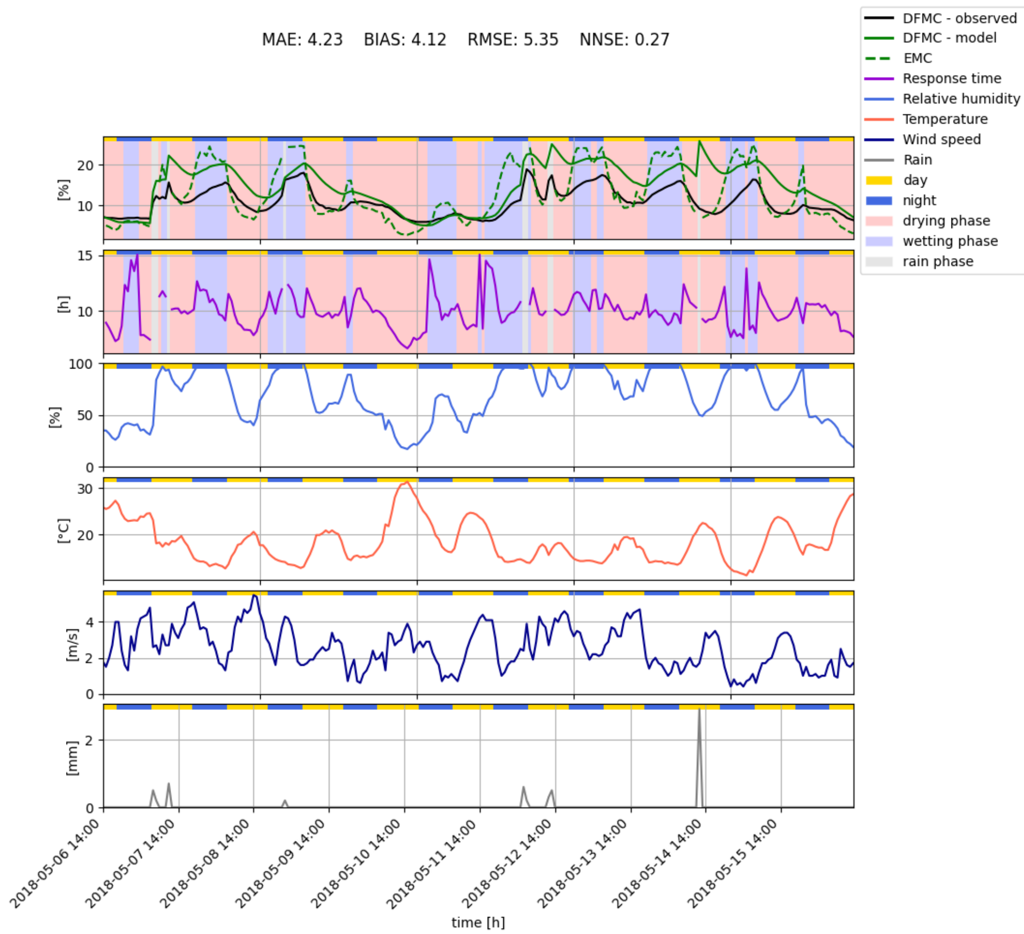

Figure 9: Mixed samplings, Summer Cluster - worst time series in terms of Mean Absolute Error (MAE). The other Goodness-of-Fit measures (bias, Root Mean Square Error and Normalized Nash-Sutcliffe) are also reported.

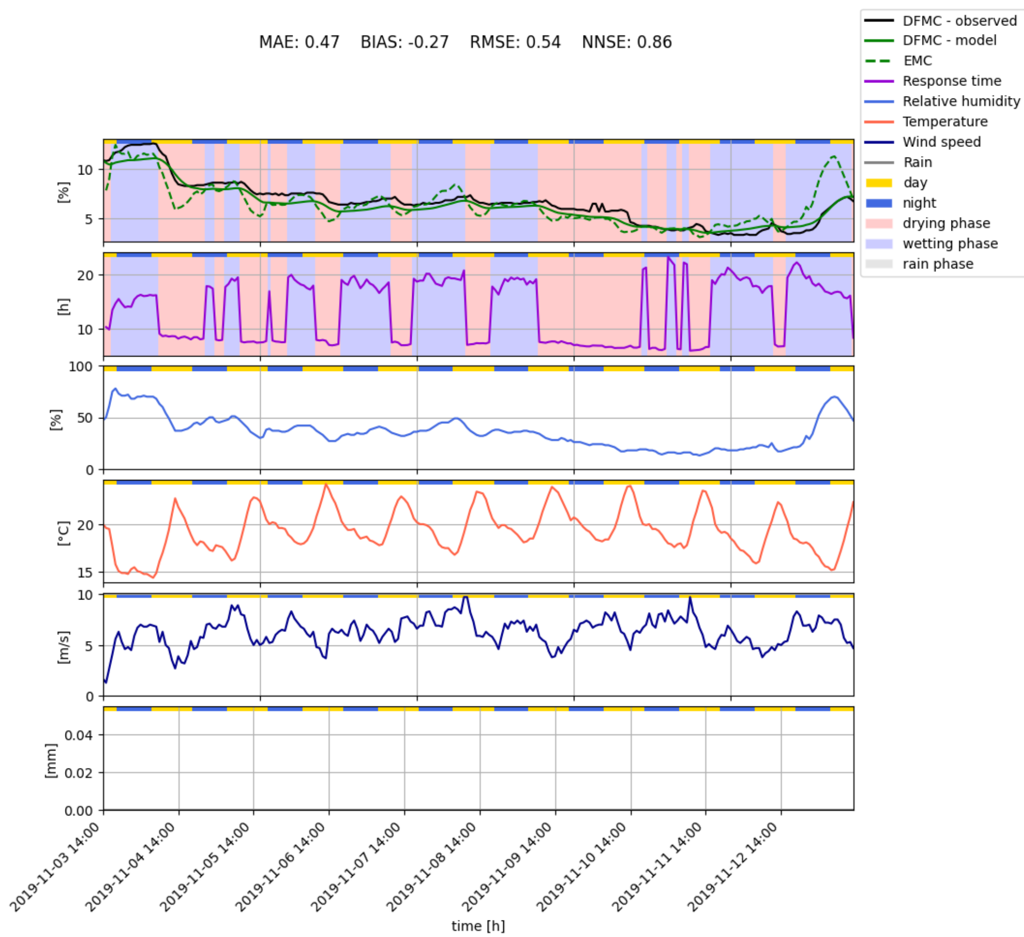

Figure 10: Mixed samplings, Winter Cluster - best time series in terms of Mean Absolute Error (MAE). The other Goodness-of-Fit measures (bias, Root Mean Square Error and Normalized Nash-Sutcliffe) are also reported.

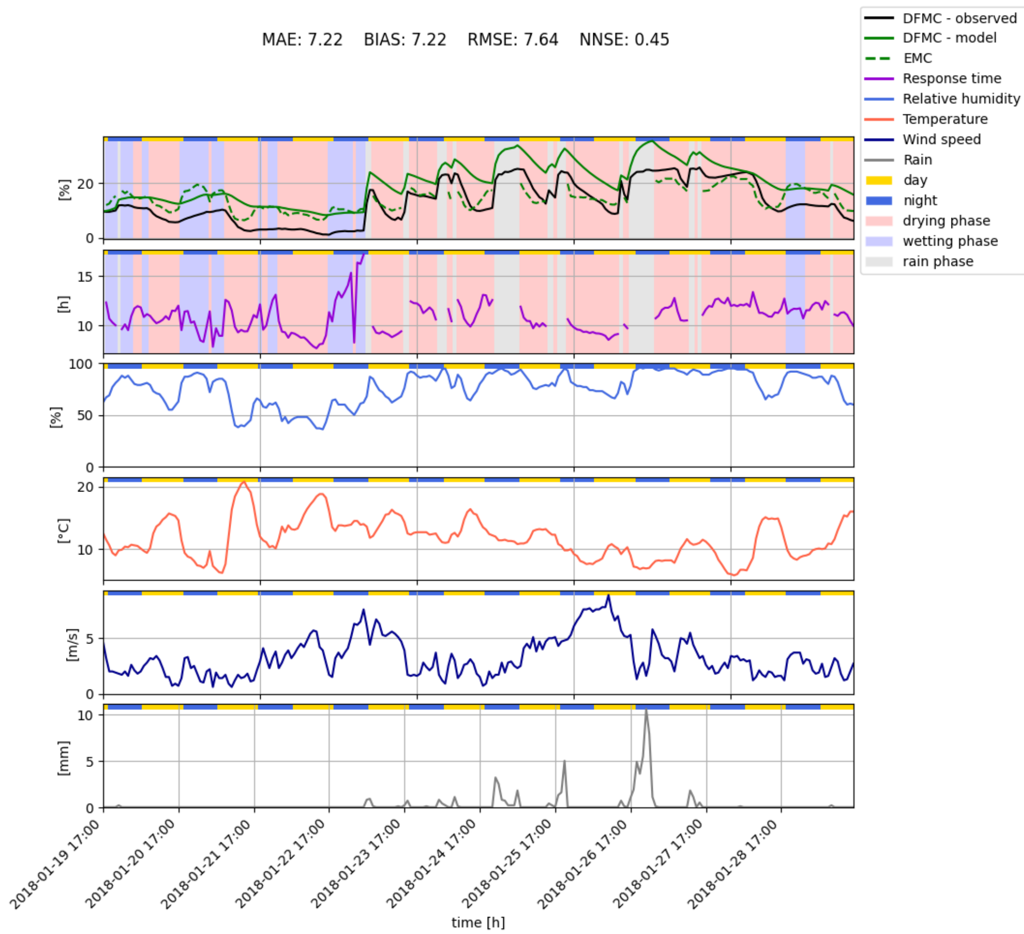

Figure 11: Mixed samplings, Winter Cluster - worst time series in terms of Mean Absolute Error (MAE). The other Goodness-of-Fit measures (bias, Root Mean Square Error and Normalized Nash-Sutcliffe) are also reported.

Ecology and the Environment 19, 387–395. doi:10.1002/fee.2359.